

Supplementary Material and Figures to

A stomatin dimer modulates the activity of acid-sensing ion channels

Janko Brand^{1,2}, Ewan St. J. Smith³, David Schwefel¹, Liudmilla Lapatsina³, Kate Poole³, Damir Omerbašić³, Alexey Kozlenkov³, Joachim Behlke^{1,4}, Gary R. Lewin³ and Oliver Daumke^{1,5}

¹Max-Delbrück Center for Molecular Medicine, Crystallography Department, Robert-Rössle-Straße 10, 13125 Berlin, Germany ²Freie Universität Berlin, Institute of Chemistry and Biochemistry, Takustrasse 6, 14195 Berlin, Germany ³Max-Delbrück Center for Molecular Medicine, Department of Neuroscience, Robert-Rössle-Straße 10, 13125 Berlin, Germany ⁴(† 5.4.2011) ⁵Institute of Medical Physics and Biophysics, Charité, Ziegelstraße 5-9, 10117 Berlin, Germany

Correspondence to:

Oliver Daumke, Max-Delbrück Center for Molecular Medicine, Robert-Rössle-Strasse 10, 13125 Berlin, Germany. Tel.: 0049-30-94063425; Fax: 0049-30-94063814; E-mail: oliver.daumke@mdc-berlin.de

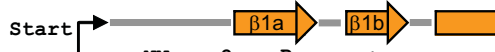
Or

Gary R. Lewin, Max-Delbrück Center for Molecular Medicine, Robert-Rössle-Strasse 10, 13125 Berlin, Germany. Tel.: 0049-30-9406 2430; Fax: 0049-30-9406 2793; E-mail: glewin@mdc-berlin.de

Supplementary Figure 1

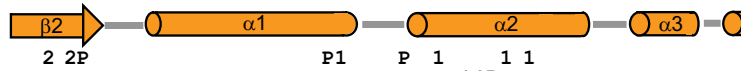
A

mmSTOM	MSDKRQSSHV	QSQRIPESFR	ENSKTELGAC	GWLLVAASFF	FVITTFPTSI	WICLKIVKEY	60
mmSLP3	-----MDS	PEKLEKNNLV	GTNKSRLGVC	GWLLFPLSL	LMLVTFPISV	WMCLKIKKEY	53
ceMEC2	VKKEKQAEKD	VEKNGKKEEK	ANIQNEFGVC	GWLLTILSYL	LIFFTLPISA	CMCIKVVQEY	147
phSTOM	-----	-----MMFAT	NFVTSIILL	FILLFLAS--	--AIKIVKEY		31
mmPODO	GPGEETEVV	ALLESERPPEE	GIKPSGLGAC	EWLLVLASLI	FLIMTFPFSI	WFCIKVVQEY	133
mmSLP2	-----MLAR	AARGTGALLL	RGSVQASGRV	PRRASSGLPR	NTVTLFVPPQ		44
mmSLP1	LGSQKGCLSP	EPGSVGPAD	APESWPSCLC	HGLVSVLGF	LLLLTFPTSG	WFALKIVPTV	85
hsFLOT1	-----	-----	-----	-----	-----MFT	GGPNEAMVVS	14
mmFLOT2	-----	-----	-----	-----	-----MGNCHT	VGPNEALVVS	16



			LI91, 92AA	NN	2	P	1		
				●●	●		●		LI109D
mmSTOM	ERVIIIFRLGR	LIQGGAKGPG	LFFILPCIDS	LIKVD-MRTI	SFDIPEQEV	TKDSVITISVD			119
mmSLP3	ERVVVFRLGR	IQADKAKGPG	LILVLPCLDV	FVKVD-LRTV	TCNIPPEQIL	TRDSVITISVD			112
ceMEC2	ERVVIFRLGR	LMGGAKGPG	LFFIVPCIDT	YRKVD-LRVL	SFVPPQEV	SKDSVITISVD			206
phSTOM	ERVVIFRLGR	VVG--ARGPG	LFFIIPIFEK	AVIVD-LRTQ	VLDVPEQEV	TKDNVPTISVD			88
mmPODO	ERVVIFRLGH	LLPGRAGGPG	LFFFLPCLDT	YHKVD-LRLQ	TLFIPFHEVV	TKDMEITISVD			192
mmSLP2	ERVVIFRMGR	FHR--ILEPG	LNVLPVLDL	IRVQSLKEI	VNVVPEQSAV	TLDNVITISVD			102
mmSLP1	ERMIVFRLGR	IRN--PQGG	MVLLLPFIDS	FORVD-LRTR	AFNVPPCKLA	SKDGAVLISVD			142
hsFLOT1	GFQRS--PPV	MVAGGR--VF	VLPCTQQIQR	ISLNT----	LTLNVKSEKVV	TRHGPIISVT			66
mmFLOT2	GGCCGSDYKQ	YVFGGW--AW	AWWCISDTQR	ISLEI----	MLQPRCEDVE	TAEQVALISVT			70

● R184C



									● LI145D
mmSTOM	GVVYIRVQN--	-ATLAVAN--	-----ITNA	DSAPRLAQT	TLRNALGKN	LSQILSDREA			169
mmSLP3	GVVYIRIYS-	-AVSAVAN--	-----VNDV	HQATFLAQT	TLRNVLGTQT	LSQILSGREA			162
ceMEC2	AVVYFRISN-	-ATLSVTN--	-----VEDA	ARSTKLAQT	TLRNILGKTI	LAEMLSDEEA			256
phSTOM	AVVYFRVVD-	-PVKAVTQ--	-----VKNY	IMATSQISQT	TLRSVIGQAH	LDELLSEREK			138
mmPODO	AVCYRYMEN-	-ASLLSS--	-----LAHV	SKAIQFLVQT	TKRRLLAHRS	LFEILLERKS			242
mmSLP2	GVLYLRIMD-	-PYKASYG--	-----VEDP	EYAVTQLAQT	TMRSELCKLS	LDKVFRERES			152
mmSLP1	ADVCFRIWD-	-PVLISVMA--	-----VKDL	NTATRMTAHN	AMTKALLRRP	LQETIQEKLK			192
hsFLOT1	GIAQVKIQGQ	NKEMLAAACQ	MFLGKTEAEI	AHIALETLEG	HORAIMAHMT	VEEIVYDRQK			126
mmFLOT2	GVAQVKIMT-	EKELLAVACE	QFLGKNVQDI	KNVVLTLEG	HLSRLGTLT	VEQIYODRQ			129

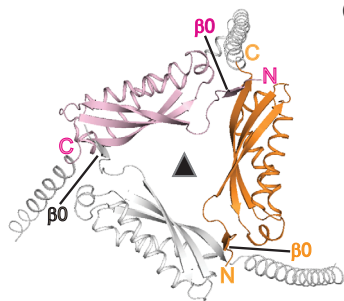
● R239H



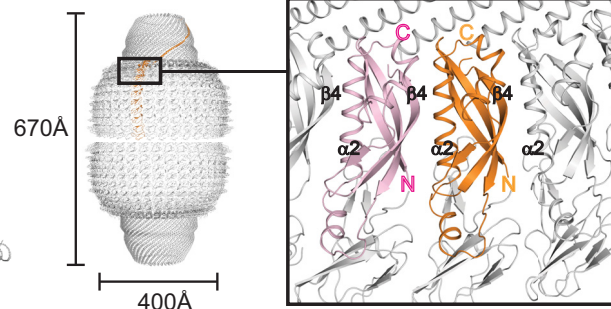
									● T182W
									● V197P
mmSTOM	IAHMQSTLD	DATDDWGIKV	ERVEIKDVKL	PVQLORAMAA	EAEAAREARA	KVIAAEGEMN			229
mmSLP3	IAHMQTLTD	DATELWGIKV	ARVEIKDVRI	PVQLORSMAA	EAEAAREARA	KVLAEGEMN			222
ceMEC2	ISHMQSTLD	EATEFPWGVK	ERVEVKDVRL	PVQLORAMAA	EAEAAREARA	KVIVAEGEQK			316
phSTOM	INMQLQRIID	EATDPWGIKV	TAVEIKDVEL	PAGMOKAMAR	QAEABRERRA	RITLAEERQ			198
mmPODO	IADQVKVAID	AVTCIWIQIKV	ERVEIKDVRL	PAGLQHSIAV	EAEAQRQAKV	RVIAAEGEKA			302
mmSLP2	LNANIVDAIN	QAADCWGIK	LRVEIKDIHV	PVRVRESMQM	QVEAERRKRA	TVLESEGTRE			212
mmSLP1	IGDQLLEIN	DVTRAWGLEV	DRVELAVEAV	LQPPDLSLTV	PSLDSLTLQL	ALHLLGSMN			252
hsFLOT1	ESEQVFKVAS	SDLVNMGIKSV	VSYTLKDIHD	DQDYLSLQK	ARTAQVQKDA	RIGEAFAKRD			186
mmFLOT2	EAKLIREVAA	PDVGRMGTEI	LSFTIKDVYD	KVDYLSLQK	TQTAVVQRDA	DIGVAEARD			189

mmSTOM	ASRAIKKESM	VITESPAALQ	LRYLQTLTIT	AAEKNSTIVF	PLPVDMLQGI	MGSNH-----	284
mmSLP3	ASKSKKESM	VLAESPVALQ	LRYLQTLTIV	ATEKNSTIVF	PLPMNILEGI	GGISYGNKK	382
ceMEC2	ASRAIKKAAE	VIAESPVALQ	LRYLQTLNSI	SAEKNSTIVF	PFPLDLISAF	LQRTPPKVEE	276
phSTOM	AAEKREAAE	IIEHPMALQ	LRFLQTLISDV	AGDKSNVIVL	MLPMEMLKLF	KSLSDAAEAY	258
mmPODO	ASESRMAAE	ILSGTPAAVQ	LRYLHHTLQSI	STEKPATVVL	PLPVDMLSL	SSPGNRAQGS	362
mmSLP2	SAINVAEGK-	KQAQILASEA	EKAEQINQAA	GEASAVLAKA	KAKAEATRIL	AGALTOHNGD	271
mmSLP1	SAVGRVPSPG	PDTLEMINEV	EPPASLAGAG	AEPSPKQVVA	EGLTALQOP	LSEALVSQVG	302
hsFLOT1	AGIREAKIKQ	EKVSAYQLSE	TEMAKAQRDY	ELKRAAYDIE	VNTRRAQADL	AYQLQVAKTK	246
mmFLOT2	AGIREAECKK	EMLDVKFMAD	TKTADSKRAE	ELQKSAFSEE	VNIKTAEAOQ	AYELQGAREQ	249

B



C

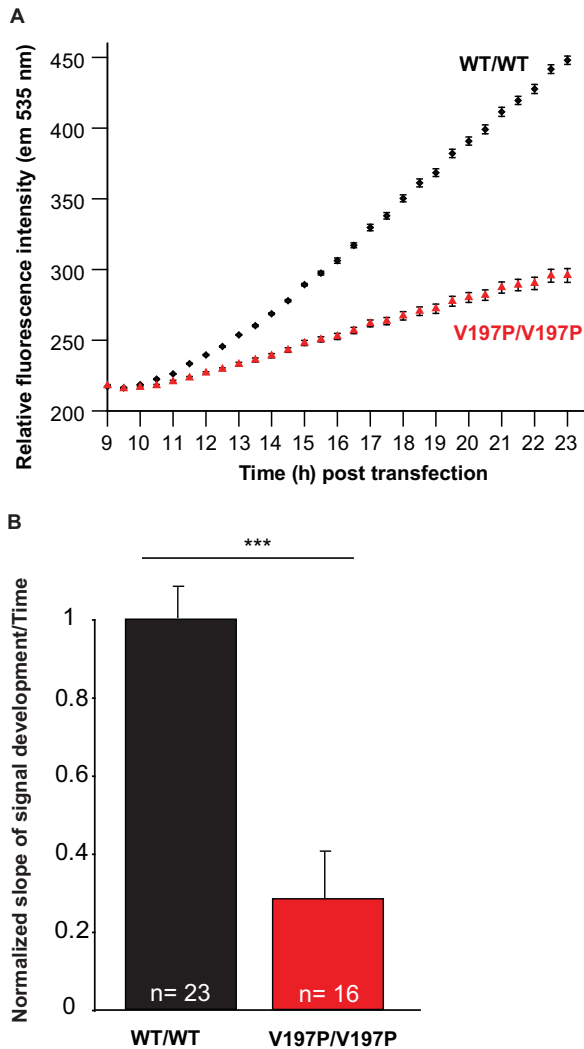


Suppl. Fig. 1: Sequence alignment and oligomerization of SPFH domain proteins

A) Sequences of mouse stomatin (Expasy accession number P54116), mouse STOML-1 (Q8CI66), mouse STOML-2 (Q99JB2), mouse STOML-3 (Q6PE84), mouse podocin (Q91X05), human Flotillin 1 (O75955), mouse Flotillin 2 (Q60634) and ph stomatin (O59180) were aligned using ClustalW (Thompson et al., 1994), and the alignment was manually adjusted. Secondary structure elements are shown on top. The following residues are indicated: D - dimerization interface, 1 - oligomerization interface-1, 2 - oligomerization interface-2, P - hydrophobic pocket. Selected mutation in MEC-2 causing touch insensitivity in *C. elegans* (Chalfie and Sulston, 1981; Zhang et al., 2004) are indicated in pink.

B, C) Oligomerization of SPFH domain proteins. (B) For ph stomatin (pdb 3BK6), a trimeric assembly was found where residues N-terminal of the stomatin domain form a β -strand which contacts the C-terminus of the next monomer. (C) The SPFH domains of the major vault protein (MVP, pdb 2ZUO) within the vault are stacked next to each other via lateral contacts of $\alpha 2$ and $\beta 4$. The N- and C- termini of the MVP SPFH domain are not involved in the assembly of the higher-order oligomers.

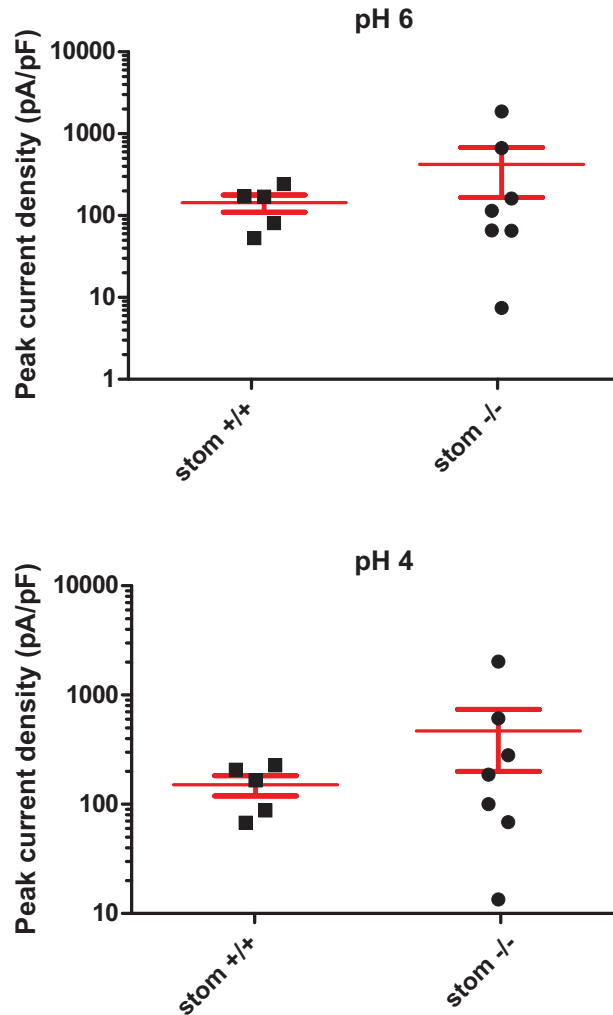
Supplementary Figure 2



Suppl. Fig. 2: BiFC time course experiments

HEK cells were co-transfected with plasmids encoding stomatin fused to N- and C-terminal fragments of YFP. Relative fluorescence intensity was monitored 8 h after transfection over 16 hours. (A) Representative results for stomatin/stomatin (n=3) and the stomatin V197P/V197P mutant (n=5) from parallel experiments. (B) The slope of the increase in relative fluorescence intensity over time was determined by a linear fit. Data of the V197P mutant were normalized to stomatin. n = number of individual transfections. *** p < 0.001 according to two tailed T-test.

Supplementary Figure 3



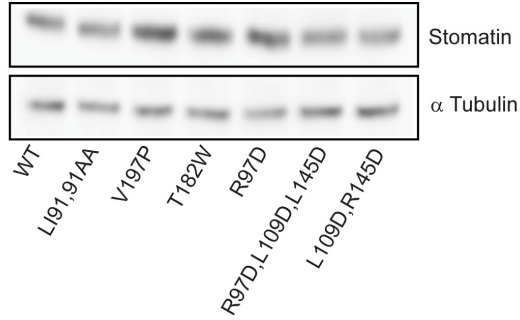
Suppl. Fig. 3: ASIC3-mediated currents in adult mouse fibroblasts.

Tail derived mouse adult fibroblasts from wild type and *stomatin*^{-/-} mice were transfected with an ASIC3 encoding plasmid and an eGFP expressing plasmid. Proton-induced currents were recorded to stimuli of pH 4.0 and pH 6.0 in GFP-expressing cells. Each dot represents one cell measurement and the red lines show mean \pm SEM. Fibroblasts were obtained from 2 wild type and 2 *stomatin*^{-/-} mice.

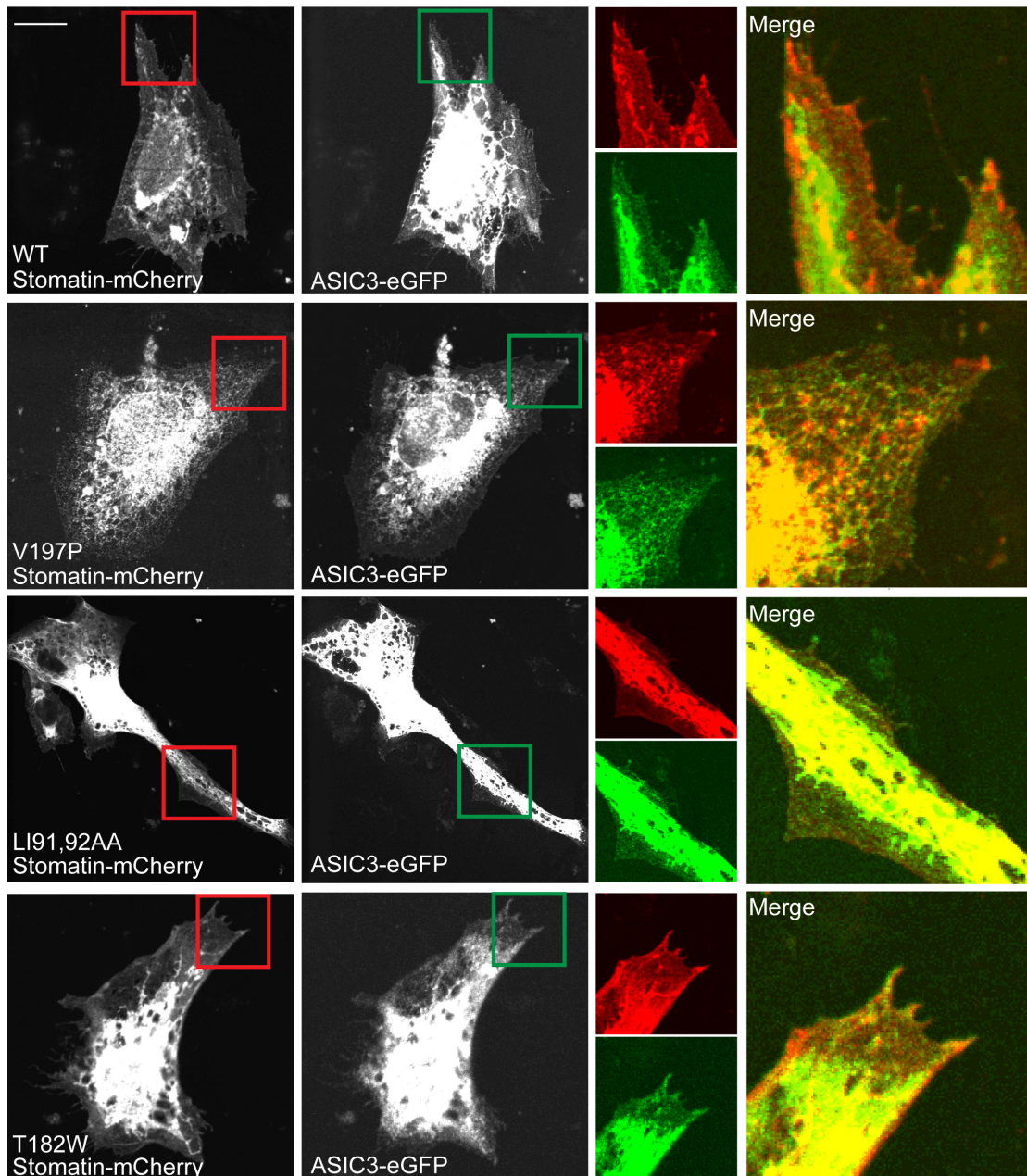
In agreement with our previous results, ASIC3-currents were on average larger in *stomatin*^{-/-} fibroblasts compared to wild type cells, but the difference was not significant, according to Student's T-test. We found that many GFP expressing cells of both genotypes failed to exhibit any ASIC3-like current, perhaps indicating that channel trafficking to the membrane is intrinsically different in primary mouse fibroblasts compared to CHO cells.

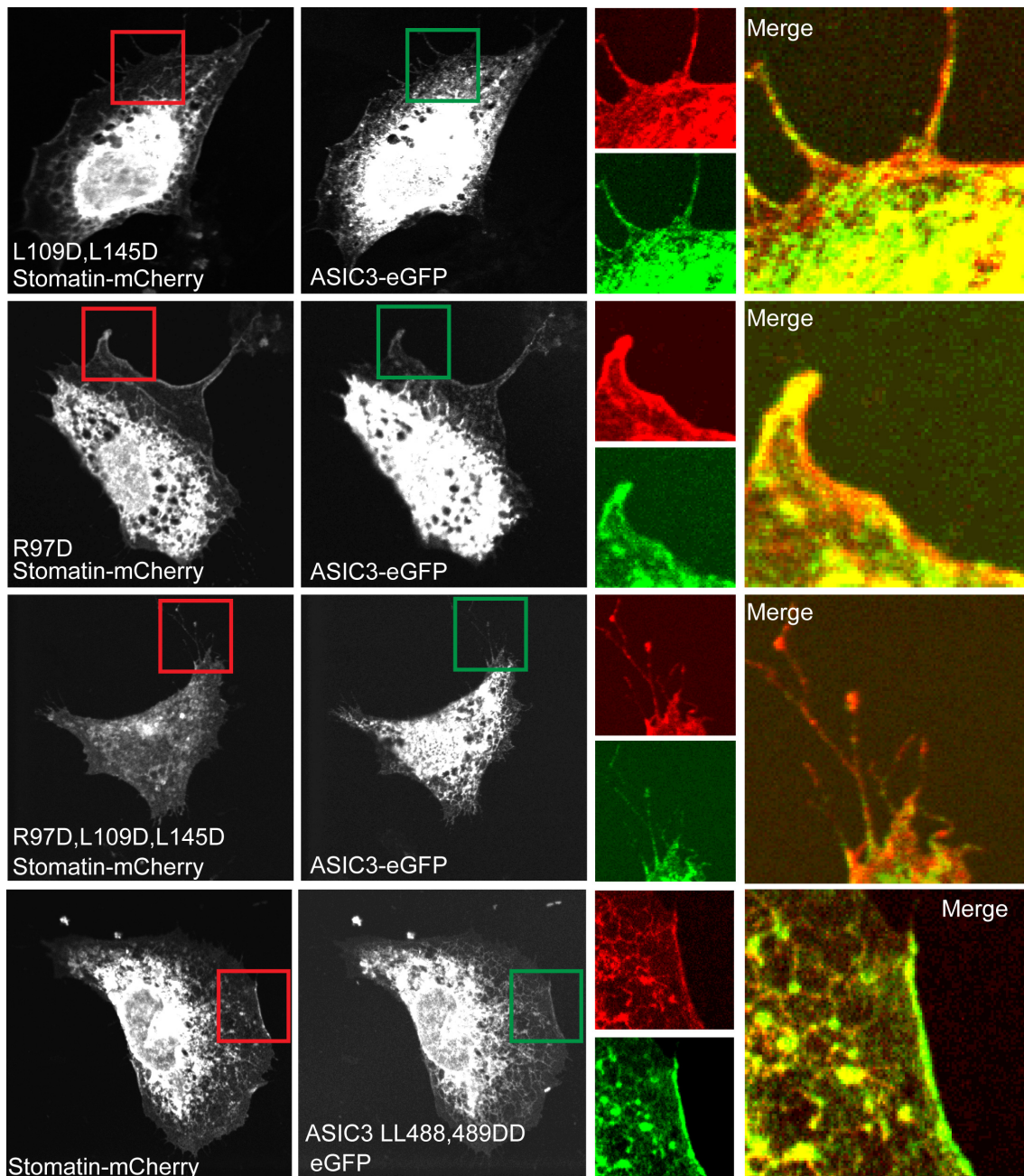
Supplementary Figure 4

A



B



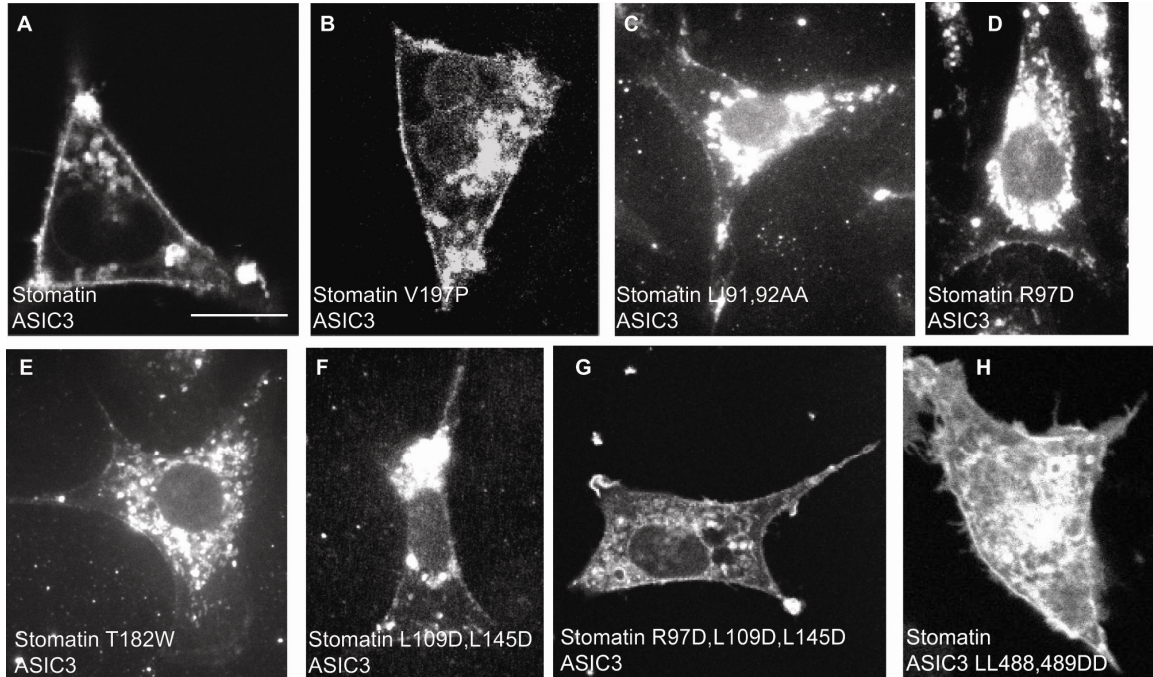


Suppl. Fig. 4: Cellular localization and expression of stomatin mutants in CHO cells

A) Western blot analysis of CHO cells transfected with Myc-His stomatin plasmids, using an anti-Myc and anti-tubulin antibody as loading control, showing comparable expression levels for all mutants.

B) CHO cells were grown to a density of 60% before co-transfection with plasmids containing mouse stomatin-mCherry or the indicated stomatin mutants and eGFP-ASIC3 or the indicated mutants. 24 h post transfection, cells were fixed and analyzed by confocal microscopy using the ImageJ software. Representative cells are shown. Sections marked by red or green boxes are merged and shown magnified on the right. The scale bar represents 20 μm .

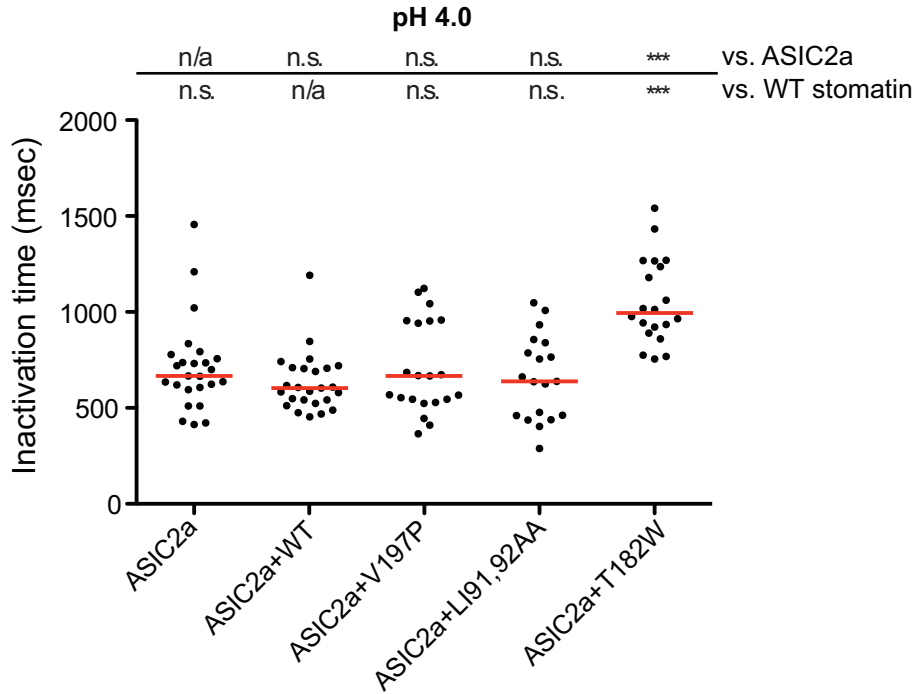
Supplementary Figure 5



Suppl. Fig. 5: BiFC microscopy of stomatin and ASIC3 in CHO cells.

CHO cells were co-transfected with plasmids encoding ASIC3 fused to a C-terminal fragment of YFP and stomatin fused to an N-terminal fragment of YFP. 24 h post transfection, cells were subjected to live cell imaging using epifluorescence microscopy. For all stomatin constructs, co-localization with ASIC3 in perinuclear structures and at the plasma membrane was visible (A-G). Also the LL488,489DD mutant of ASIC3 similarly co-localized with stomatin. The white scale bar corresponds to 20 μm.

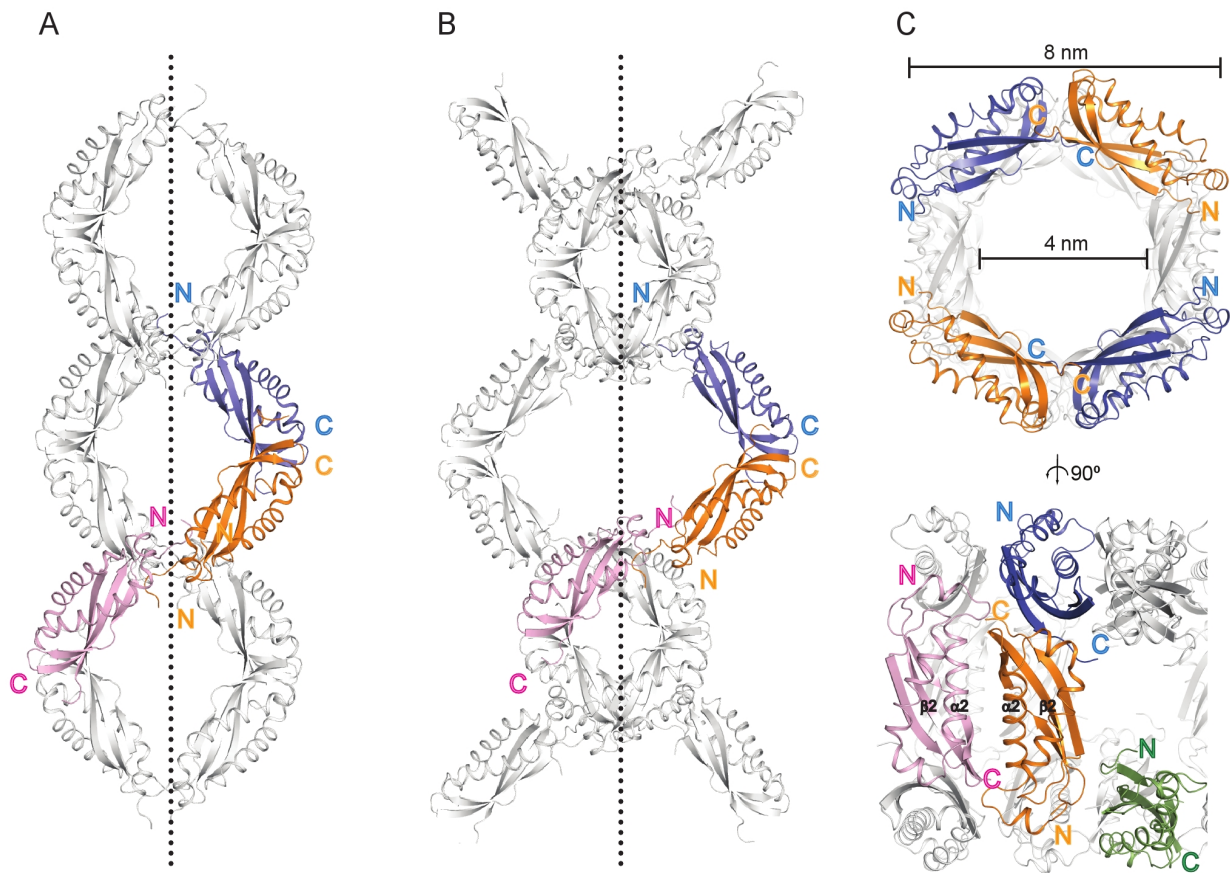
Supplementary Figure 6



Suppl. Fig. 6: ASIC2a inactivation at pH 4.0

Dot plots of inactivation time of ASIC2a at pH 4.0. Each dot represents one cell measurement, and the red lines show the median for each data set. The Kruskal-Wallis test followed by Dunn's post test and statistical comparisons of inactivation time compared to ASIC2a expressed alone and ASIC2a co-expressed with stomatin or the indicated mutants is shown. n/a, not applicable; n.s., not significant; ***, $p < 0.001$.

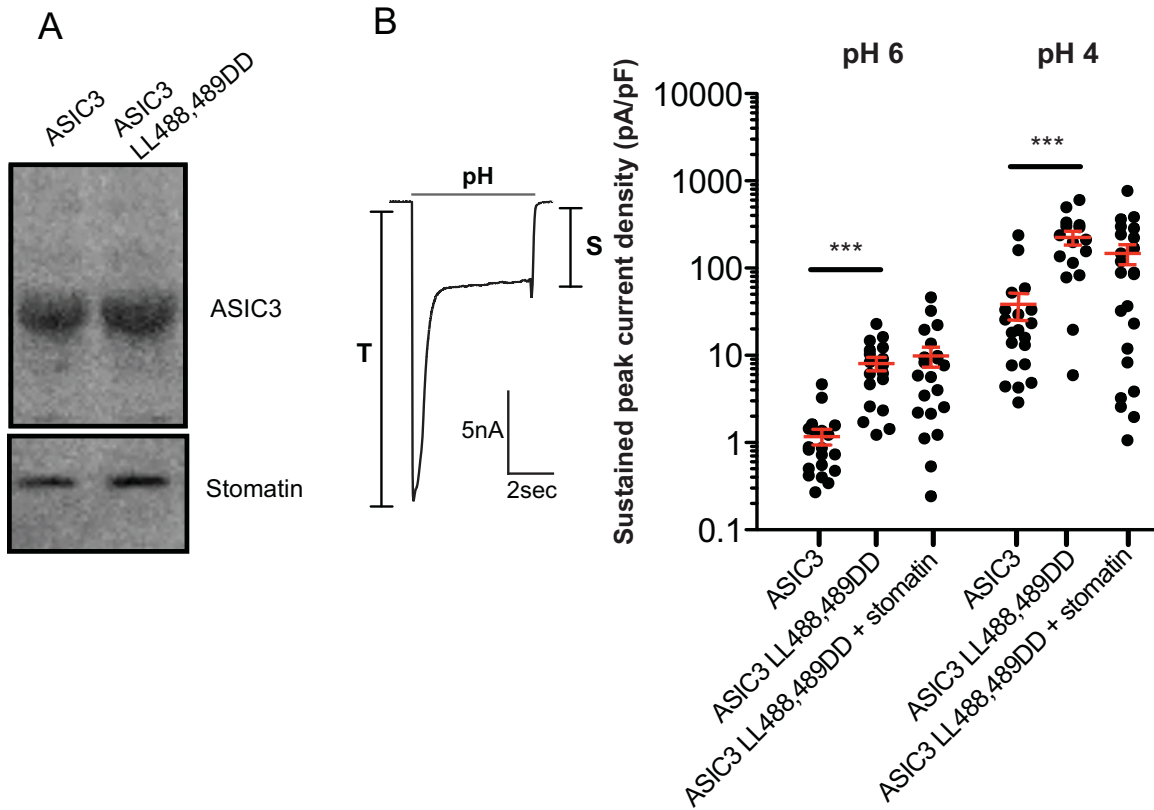
Supplementary Figure 7



Suppl. Fig. 7: Crystal packing of the mouse stomatin domain constructs

In all three crystal forms, a stomatin dimer with a C-terminal dimerization interface was observed. In crystal form 1 (A) and 2 (B), the dimers show an intertwined helical crystal packing, formed by additional contacts of the N-terminal loop preceding the stomatin domain (including Leu91 and Ile92) with the hydrophobic pocket of the adjacent dimer. In (A), the dimers form a homogeneous helix, whereas in (B), the helix is bulky. This difference originates from the flexibility of the N-terminal loops. (C) 3D figure showing the arrangement of stomatin dimers in crystal form 3, as seen in Fig. 6B. For viewing, the latest version of the freely available Adobe Reader 9 should be installed. Move the cursor over the figure and use left button to activate the 3D-mode. Use mouse left button for rotation, left button / shift for zoom function and left button / ctrl for translation. Preset views are available in the Toggle menu tree. To return to Supplementary Figure 3, use right mouse button and "Disable 3D". In crystal form 3, a tubular oligomeric arrangement is established by symmetric contacts of the stomatin domain via interface-1 and 2. Our mutagenesis data and the surface conservation plots might indicate that higher-order stomatin assembly proceeds in a similar fashion as in crystal form 3. It might also involve hetero-oligomerization between different stomatin members (Lapatsina *et al.*, 2012; Mairhofer *et al.*, 2009). Both N- and C-termini of stomatin point towards gaps in the tubular oligomers. From the crystal structure, it is unclear whether the termini would further extend to the exterior or interior of the tubular oligomer.

Supplementary Figure 8



Suppl. Fig. 8: Functional characterization of the ASIC3 LL488,489DD mutant

(A) Similar levels of ASIC3 and ASIC3 LL488,489DD were co-immunoprecipitated by Myc-tagged stomatin.

(B) Overexpressed ASIC3 LL488, 489DD in CHO cells shows increased transient (T) and sustained (S) currents. The maximal sustained current amplitude was determined as indicated on the left. The ASIC3 LL488, 489DD mutant showed increased sustained (S) current amplitudes compared to ASIC3 which were not affected by stomatin co-expression. ***, $p < 0.001$

References exclusively used in the Supplementary Material

Thompson JD, Higgins DG, Gibson TJ (1994) CLUSTAL W: improving the sensitivity of progressive multiple sequence alignment through sequence weighting, position-specific gap penalties and weight matrix choice. *Nucleic Acids Res* **22**: 4673-4680

Zhang S, Arnadottir J, Keller C, Caldwell GA, Yao CA, Chalfie M (2004) MEC-2 is recruited to the putative mechanosensory complex in *C. elegans* touch receptor neurons through its stomatin-like domain. *Curr Biol* **14**: 1888-1896